Simulation of a horizontal axis tidal turbine for direct driven reverse-osmosis desalination

Greco, F.; Jarquìn-Laguna, A.

Publication date
2019

Document Version
Final published version

Published in
Advances in Renewable Energies Offshore - Proceedings of the 3rd International Conference on Renewable Energies Offshore - RENEW 2018

Citation (APA)
Greco, F., & Jarquìn-Laguna, A. (2019). Simulation of a horizontal axis tidal turbine for direct driven reverse-osmosis desalination. In C. G. Soares (Ed.), *Advances in Renewable Energies Offshore - Proceedings of the 3rd International Conference on Renewable Energies Offshore - RENEW 2018* (pp. 181-188). CRC Press / Balkema - Taylor & Francis Group.

Simulation of a horizontal axis tidal turbine for direct driven reverse-osmosis desalination.

F. Greco & A. Jarquìn-Laguna
Delft University of Technology, Delft, Netherlands

ABSTRACT: Desalination of seawater from renewable energy sources is without doubt an appealing solution to face water scarcity issues in coastal areas. In particular, tidal energy technologies offer high potential to be integrated with existing desalination technologies. This paper contributes to the idea of using a horizontal axis tidal turbine for direct driven reverse-osmosis seawater desalination without intermediate electrical power conversion. In combination with a positive displacement pump and RO membranes, a back-pressure valve is employed at the brine exit to induce a suitable pressure in the system while keeping a variable speed operation of the rotor. A time-domain numerical model is used to simulate and compare the dynamic response of a passive and an active controlled valve configuration. Intermediate results are given for a 300kW system under turbulent current conditions.

1 INTRODUCTION

The use of renewable energy to desalinate seawater is a fundamental attractive idea to face the current challenge of water scarcity, especially in coastal areas and small islands which are the most affected by water resources issues. On one hand, the reduced area, shortage of natural resource and natural vulnerability cause problems of both water quantity, due to the absence or scarcity of permanent fresh water, and water quality due to seawater intrusion or pollution. On the other hand, isolation limits their availability to import low cost fresh water and/or fuel required to power desalination systems. However, coastal places can take advantage of their proximity to seawater sources to cover their fresh water needs. The use of renewable sources available in situ to power desalination is indeed required to limit the environmental impact of fossil fuel CO_2 emissions. The emissions from fossil fuel-powered desalination are between 1.4 and 1.8 kg per cubic meter of fresh water (Elimelech & Phillip, 2011). Although most solutions address the use of solar and wind energy technologies, covering the 81% of the renewable powered desalination around the world (Mizutani, 2016), there is high potential from other offshore renewable sources such as tidal and wave energy to be integrated with existing desalination technologies (Ling et al., 2017), (Folley & Whittaker, 2009), (Corsini et al., 2015). Other studies refer also to the use of hydro power for desalination, but mainly in combination with other renewable sources and as a storage or with fluctuation absorption purposes (Akash & Mohsen, 1998), (Slocum et al., 2016).

Tidal energy is a vast and clean energy source that has the advantage of being far more predictable than other renewable energy sources like solar and wind (Cave & Evans, 1984). From the existing tidal current energy extraction devices, horizontal axis turbines are the most popular (Goundar & Ahmed, 2013). Showing many similarities with the horizontal axis wind turbine, its development can benefit from the advantages in the technologies in the wind energy industry (Rourke et al., 2010).

Regarding desalination technologies, reverse osmosis (RO) is the most common membrane-based desalination system, and its popularity its increasing due to the reduced cost per m^3 of water produced when compared to other desalination technologies. RO is one of the less energy consuming desalination processes, requiring about 3-10 kWh of electric energy per m^3 of freshwater produced from seawater (Ma & Lu, 2011). The energy consumption is mainly due to pump the feed water up to a pressure high enough to overcome the osmotic pressure difference between the two sides of the membrane. When this occurs, pure water is forced to pass through the membrane (permeate), while the salts, ions and small particles are retained and exit as brine (concentrate). A valve is required on the concentrate line to provide a resistance to the flow in order to allow the pressure build up.

Membranes can be designed in many different configurations. The type selected in this study is a

spiral wound membrane, that is essentially made by flat sheets coiled around a perforated collection pipe. This design offers the advantages of lower replacement costs, simpler plumbing system, easier maintenance and greater design freedom than other configurations, and thus it is one of the most commonly used for seawater desalination (DOW, 2013).

This paper elaborates on the idea to desalinate seawater using the tidal currents, in which the energy harnessed by a horizontal axis turbine is directly used by a rotor-pump combination to pressurize seawater into the RO membranes. In contrast to conventional approaches, no intermediate electrical power conversion is needed, making it more simple, robust and in principle more suitable for small and off-grid applications. One of the main objectives of the proposed solution is to understand the possibilities and limitations of reverse osmosis desalination under the influence of dynamic excitations from the tidal current resource. A time-domain numerical model is constructed to simulate the coupled response of both the rotor and reverse osmosis membranes under turbulent current conditions.

2 DIRECT-DRIVEN REVERSE OSMOSIS DESALINATION

A schematic of the direct-driven RO desalination system is shown in Figure 1: the kinetic energy from tidal currents is extracted by the horizontal axis rotor and transmitted to the high-pressure water pump; the rotor and the pump are directly connected. The pressurized sea water is then sent as feed in the reverse osmosis desalination process. The fresh water is collected at the permeate side while the concentrate goes through the backpressure valve.

Two different configurations of direct-drive RO desalination are analyzed. In each configuration the torque characteristics of the rotor are matched in a different manner with the RO system. The first configuration considers a variable speed operation of the turbine rotor in a passive manner through the RO membrane characteristics and a fixed valve setting. The second configuration aims to keep an optimal variable speed operation of the rotor by manipulating the opening and closing of the concentrate valve linked to the RO system.

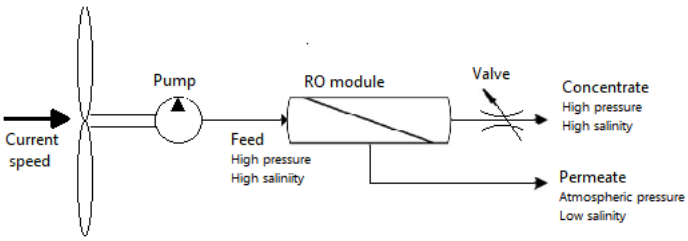

Figure 1. Schematic of the system.

3 MATHEMATICAL MODEL

3.1 *Tidal turbine*

The horizontal axis tidal turbine extracts kinetic energy from the current and converts it in rotary motion. The power extracted depends on the hydrodynamic characteristics and geometry of the rotor and on the current speed. The hydrodynamic torque τ_{rotor} and the power extracted P_{rotor} can be expressed as functions of the upstream current speed $U_{current}$, the radius of the rotor R_{rot} and the non-dimensional coefficients C_τ and C_P, as follows:

$$\tau_{rotor} = \frac{1}{2} C_\tau(\lambda, \beta)\, \rho\, \pi\, R_{rot}^3\, U_{current}^2 \quad (1)$$

$$P_{rotor} = \frac{1}{2} C_P(\lambda, \beta)\, \rho\, \pi\, R_{rot}^2\, U_{current}^3 \quad (2)$$

where ρ represents the seawater density; β is the collective pitch angle, the deviation from the angle between the rotor plane and the tip chord, and λ denotes the tip speed ratio, that is the ratio of the rotor tip tangential speed to the upstream current speed:

$$\lambda = \frac{\omega_r R_{rot}}{U_{current}} \quad (3)$$

The torque and power coefficients are related by the following relationship:

$$C_P = \mathrm{C}_\tau \lambda \quad (4)$$

The non-dimensional coefficients for the tidal turbine can be obtained through the blade element momentum equations for stationary flow as described in (Batten et al., 2008) and solved with the solution method described by (Ning, 2014). The geometrical and hydrodynamic characteristics of the turbine blades were taken from (Batten et al., 2008).

3.2 *Low-speed shaft and seawater pump*

The power transmission system consists of a positive displacement pump, that is connected on the same shaft of the rotor. Therefore, the imbalance of the hydrodynamic and the pump torques causes the angular acceleration of the rotor-pump assembly considered as a rigid body, as expressed by the differential equation

$$(J_r + J_p)\frac{\mathrm{d}\omega_r}{\mathrm{d}t} = \tau_{hydro} - \tau_{pump} - B_r \omega_r \quad (5)$$

where J_r and J_p represent the mass moments of inertia of the rotor and the pump, respectively. The last term on the right represents the viscous friction torque, expressed as a linear function of the rotor shaft viscous damping coefficient B_r.

The pump torque can be calculated once the volumetric displacement V_d of the pump is known, that denotes the volume of fluid that is displaced at every rotation, in m^3/rad. The pump model is based on quasi-steady linear relations which describe both the transmitted torque and the net generated volumetric

flow rate (Merritt, 1967). The transmitted pump torque is a function of the pressure difference across the pump Δp_p and of the rotational speed of the rotor, according to the relationship:

$$\tau_{pump} = V_d \Delta p_p + C_{f,p} V_d \Delta p_p + B_p \omega_r \quad (6)$$

The coefficients B_p and $C_{f,p}$ are the damping coefficient and a friction coefficient, respectively. These coefficients are used to take into account the viscous and dry components of the friction torque. Moreover, the pump is also characterized by the volumetric flowrate that is obtained by:

$$Q_f = V_d \omega_r - C_{s,p} \Delta p_p \quad (7)$$

where the last term represents the internal leakage losses, estimated in a linear manner through the laminar leakage coefficient $C_{s,p}$.

In order to evaluate the dynamic behavior of the coupled hydraulic tidal turbine-RO membrane, the configuration of the system analyzed envisages that the flowrate Q_f is directly fed to the membrane. The dynamics of the hydraulic lines and additional losses through pipes are not considered.

3.3 *RO Membrane*

The reverse osmosis desalination process is based on the selective permeability of the membrane, that allows the flow of water and retains salts and ions. The solution-diffusion model can proper represent the transport across the dense RO membrane (Wijman & Baker, 1995). According to this model, permeants are first absorbed onto the membrane surface, then diffuse across its thickness and finally they are released on the other side of the membrane. The flow rate of each component per unit area that passes across the membrane is the flux.

Thus, the expression for the water flux is:

$$J_w = K_w(\Delta p - \Delta \pi) \quad (8)$$

where K_w represents the water permeability constant; Δp is the difference in pressure between the two sides of the membrane; and $\Delta \pi$ is the osmotic pressure difference.

The osmotic pressure difference depends on the effective concentration of total dissolved solid (TDS) at the membrane surface at the feed side, C_{eff}, and can be calculated as follows (Bartman et al., 2008):

$$\Delta \pi = \delta C_{eff} T \quad (9)$$

$$\frac{C_{eff}}{C_f} = a + (1-a)\left((1-R) + R\left(\frac{U_f}{U_c}\right)\right) \quad (10)$$

where T denotes the temperature in K; a is the weighting coefficient; C_f represents the feed concentration; and U is the water velocity. The subscripts f, c and p stand for the feed, concentrate and permeate respectively. The salt rejection R represents the ability of the membrane to retain the salts, expressed by:

$$R = \left(1 - \frac{c_{sl}}{c_{so}}\right) \quad (11)$$

For salt flux a similar relation to water flux is found:

$$J_s = K_s(c_{so} - c_{sl}) \quad (12)$$

where K_s represents the salt permeability constant; and $(c_{so} - c_{sl})$ is the difference in salt concentration between the two sides of the membrane.

Another important parameter that characterizes RO osmosis is the recovery rate RR, that represents the ratio of membrane system feedwater that emerges from the system as product water or permeate:

$$RR = \frac{Q_p}{Q_f} \quad (13)$$

3.4 *Concentrate valve*

The non-linear model used to describe the RO membrane-valve system is derived using the energy and mass balances as proposed by (Bartman, Christofides, & Cohen, 2008), considering the assumptions that water is an incompressible fluid and its density is assumed constant. Furthermore, there is no external work done on the control volume and that the inlet and outlet velocities are equal, the macroscopic energy balance around the concentrate valve reduces to:

$$\frac{\mathrm{d}}{\mathrm{d}t} E_{k,tot} = -\frac{\Delta p}{\rho} \dot{m} - E_v \quad (14)$$

where $E_{k,tot}$ represents the kinetic energy in the control volume and $\dot{m}$ the mass flow rate.

The friction losses, E_v, can be approximated as follows:

$$E_v = \frac{1}{2} e_v \dot{m} U_c^2 \quad (15)$$

by means of the friction losses factor e_v, that is a coefficient representing the valve resistance to the flow and that depends on the valve characteristics. Note that the flow velocity across the valve has been assumed equal to the concentrate flow velocity U_c.

By substituting in (14) the expressions of kinetic energy in the control volume $E_{k,tot}$ and of the mass flow rate $\dot{m}$, it is obtained:

$$\rho V \frac{d}{dt} U_c = p_{sys} A_c - \frac{1}{2} \rho e_v A_c U_c^2 \quad (16)$$

where V is the system volume and A_c denotes the concentrate pipe area, substituting the valve area. It must be noticed that since the flows exits at atmospheric pressure, the difference in pressure Δp can be reduced to the pressure of the system p_{sys}.

The valve settings can be manipulated by using an actuator that modifies the friction losses factor e_v. The dynamics of such an actuator are approximated by a first order differential equation:

$$T_v \frac{d}{dt} e_v = e_{v,ref} - e_v \tag{17}$$

where the valve constant T_v, characterizes the time response of the valve to reach the reference value $e_{v,ref}$.

3.5 *Desalination system*

In order to obtain an expression for the pressure of the system, the water flux can be also defined in terms of volumetric flow rate per unit area and the equation can be combined with equation (8) giving:

$$p_{sys} = \frac{\rho U_p A_p}{A_{tot} K_w} + \Delta\pi \tag{18}$$

where A_{tot} is the total membrane area available.

Finally, substituting last equation in equation (16), and considering the mass balance over the RO membrane and valve system:

$$U_f A_f - U_c A_c - U_p A_p = 0 \tag{19}$$

we obtain:

$$\rho V \frac{d}{dt} U_c = \frac{\rho A_c \left(U_f A_f - U_c A_c\right)}{A_{tot} K_w} + \\ + \Delta\pi A_c - \frac{1}{2} \rho A_c e_v U_c^2 \tag{20}$$

Equation (20), together with equation (9) and (10), define all the governing equations to model the RO system.

4 STEADY-STATE OPERATIONAL ENVELOPE

4.1 *Variable speed strategy*

The power capture of a tidal turbine is maximized for a particular current speed when it is able to modify its rotational speed to match optimal hydrodynamic performance. The rotor should be able to operate with a constant tip speed ratio where the maximum power coefficient is achieved for the required range of current speeds. The optimal hydrodynamic torque as a function of the rotor speed is derived by substituting equations (3) and (4) into equation (1). The following quadratic relation is obtained (Bianchi et al., 2007):

$$\tau_{hydro} = \frac{1}{2} \frac{C_{P,max}}{\left(\lambda_{C_{P,max}}\right)^3} \rho \, \pi \, R_{rot}^5 {\omega_r}^2 \tag{21}$$

For optimal operation, the transmitted torque of the pump should be in equilibrium with the hydrodynamic torque described by last equation. However, the relation between the pump torque and the rotational speed depends directly on the system pressure which is defined by the membrane characteristics and the backpressure valve settings.

In general, the equilibrium of the rotor-RO system is achieved when the torque of the pump is able to match the hydrodynamic torque at rotational speeds above the maximum torque curve. The maximum rotational speed of the rotor is given by the maximum tip speed in order to avoid cavitation.

4.2 *Operational limits and design considerations*

Once the pump size is selected according to the flow rate and rotational speed requirements, regulation of system pressure and torque is done by adjusting the valve setting. A proper design of the system requires to consider the operating limits of both membrane and turbine while operating as close as possible to optimal hydrodynamic conditions. In Figure 2 the torque-rotor rotational speed graphs are shown for the rotor and the pump-RO system

Regarding the membrane, the bottom limit is set by the minimum admissible applied pressure, that guarantees that reverse osmosis occurs; on the other side, the maximum feed pressure is related to the physical limits and resistance of the membrane. For seawater average concentration, equal to 35000 ppm,

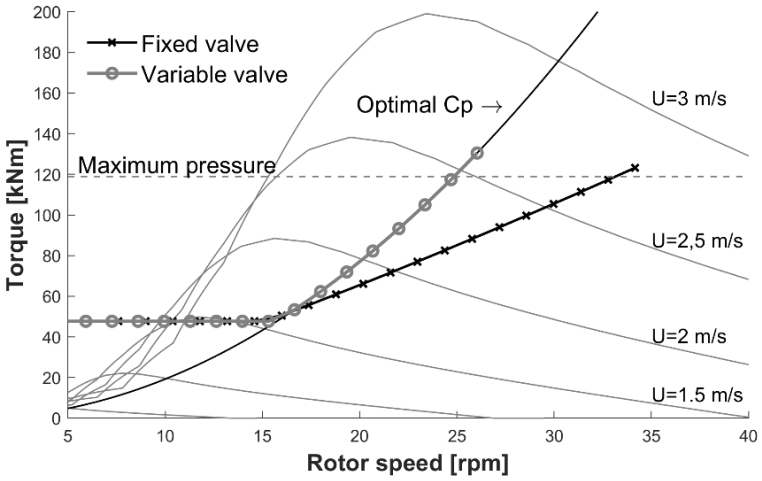

Figure 2. Hydrodynamic and pump torque over rotational speed.

osmotic pressure is around 27 bar, while the maximum pressure given for the membrane is of 69 bar. Moreover, the brine flow rate should be high enough to avoid precipitation and consequent membrane fouling but shouldn't exceed limit imposed to avoid membrane wearing and deterioration. However, in the present analysis this limitation is not considered.

In Table 1 the design values selected are summarized taking into account all previous considerations.

In Figure 2 the final resulting curves in the torque-rotational speed plot are shown for both configurations: with the fixed valve setting defined by a constant e_v, and with the varying valve setting. With the selected design, water desalination is possible for current speeds greater than 1.5 m/s. The rated current speed is given by the torque corresponding to maximum admittible pressure for the membrane resistance. The rated speed is different for the two different setting, it is 2.7 m/s in the case of the fixed valve, and 2.5 m/s in the variable valve configuration. It is possible to see in Figure 3, that the pressure of the system increases much faster in the variable valve case, bringing the system to reach the maximum limit for a slower rotational speed. Moreover, at 33 rpm, the rated rotational speed is higher when the opening valve position is fixed, than the rated 25 rpm of variable valve setting, and the working point curve remains further from the unstable area. This means that with the fixed setting configuration the range of operability and safety margin of the turbine is greater, considering that the lower value is given by the maximum torque limit. Nevertheless, in both cases there is a sufficiently wide operating window.

In Figure 4 the ideal power, the power extracted from the rotor and the power that is effectively being used to obtain the permeate are shown for both cases.

Table 1: Input and design parameter

Parameter	Value	Units
K_w	6.4E-09	s/m
A_m	15.6	m^2
A_f	0.0004568	m^2
A_c	0.0004568	m^2
A_p	0.0002726	m^2
δ	0.2641	Pa/ppm K
R	0.97	-
V	0.6	m^3
T	22	°C
ρ	1025	kg/m^3
C_f	35000	ppm
a	0.5	-
V_d	0.6	Cc/rev
e_v	1.5	-
n_{memb}	47	-
R_{rot}	5.5	m

As expected, the power captured and translated in permeate flowrate is higher in the variable opening valve position configuration. It is clear that the regulation of the valve has an important role in conditioning and controlling the performance of the system. Increasing or decreasing the opening valve position allows to modify the slope of the pump curve. When the torque slope is high the power utilization is

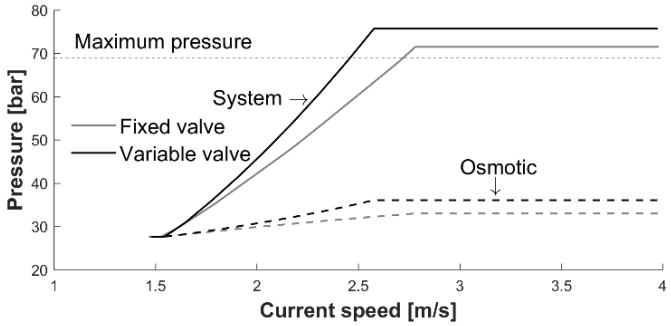

Figure 3. Steady-state operating pressures.

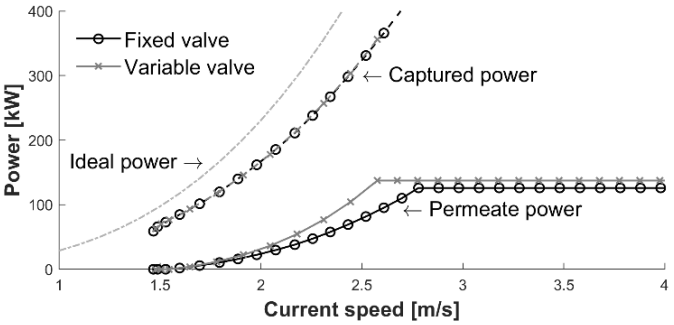

Figure 4. Steady-state power conversion.

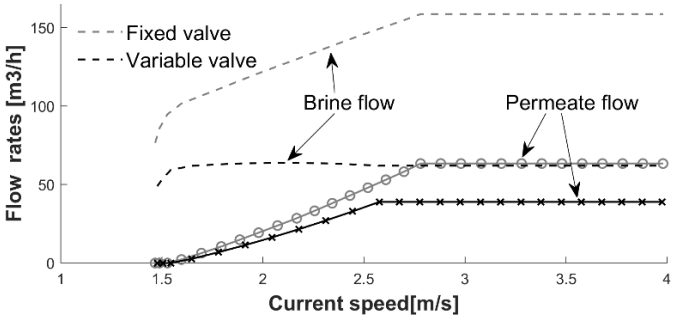

Figure 5. Steady-state operating flowrates.

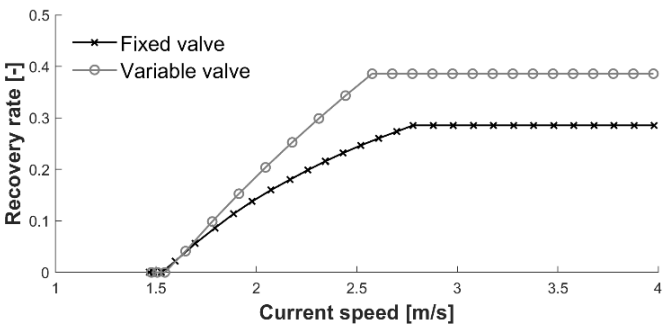

Figure 6. Steady-state RO recovery rates.

higher, but the range of rotational speed is narrower and closer to the unstable area.

In Figure 5 the feed, permeate and brine flowrates are shown as a function of the current speed. For the case of the varying opening valve position the flowrates are lower than when the valve is fixed, with an increasing gap for higher current speeds. From Figure 6, the recovery rates are higher for the fixed valve configuration because the concentrate flowrate stabilizes to a constant value around 62 m^3/h while the permeate flowrate increases with the feed. Thus, for a current velocity of 2.5 m/s, the recovery ratio is equal to 0.35 for the variable valve and 0.24 when the valve is fixed. Therefore, in the case of the fixed valve configuration permeate flowrate outcome is higher, even though there is a worse utilization of the feed than in the variable valve configuration.

5 SIMULATION OF THE DYNAMIC RESPONSE (DYNAMIC RESPONSE SIMULATION)

In order to evaluate the dynamic behavior of the proposed tidal turbine with direct-drive RO desalination, time domain simulations were performed to describe the response of the system to turbulent current speed conditions. The numerical model was implemented in the commercial software Matlab-Simulink using equations (1), (3-(7), (9), (10), (17) and (20). The system of coupled algebraic and differential equations was then solved through numerical integration using a standard ordinary differential equation (ODE) solver based on a variable time- step, explicit Runge-Kutta 4th order scheme.

The results are shown for only a preliminary case study where the current speed time series used as input has a mean value of 2.2 m/s with a turbulence intensity of 6%, (Figure 7a). This value is consistent with observed values reported in (Thomson et al., 2013). The pump sizing and valve settings were done based on a tidal turbine of 300 kW with a rotor radius of 5.5 m.

The two different configurations are analyzed and compared: in the first one the setting of the retentate valve is fixed, in the second one, the valve is adjusted in order to obtain the optimal variable speed operation of the rotor. The results of the simulation are shown for 600 seconds in Figure 7 and Figure 8.

In Figure 7b is plotted the rotor rotational speed. Following the steady-state results of section 4, the speed for the fixed setting is higher than in the variable mode. In both cases, a stable variable speed operation is observed as a function of the current speed.

In Figure 7c, the brine and permeate flowrates of the fixed valve and variable valve are shown. It is possible to observe that the permeate flowrates show the same behavior in both configurations, although the variable valve approach results in a slightly higher mean flowrate (562 l/min against 482 l/min of the fixed setting approach); on the contrary, the concentrate flowrates differ: in case of variable valve the

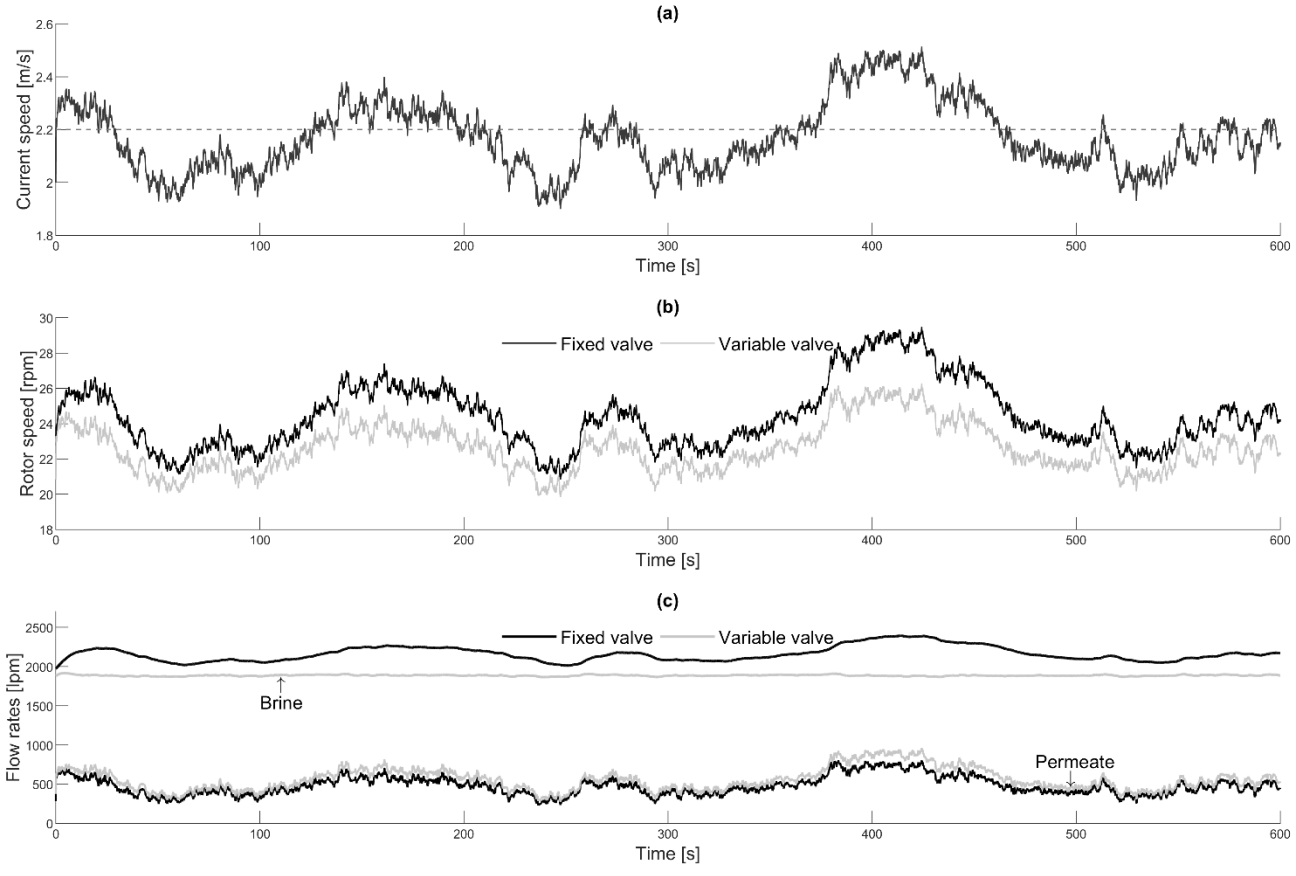

Figure 7. Current speed, rotor speed and flowrates.

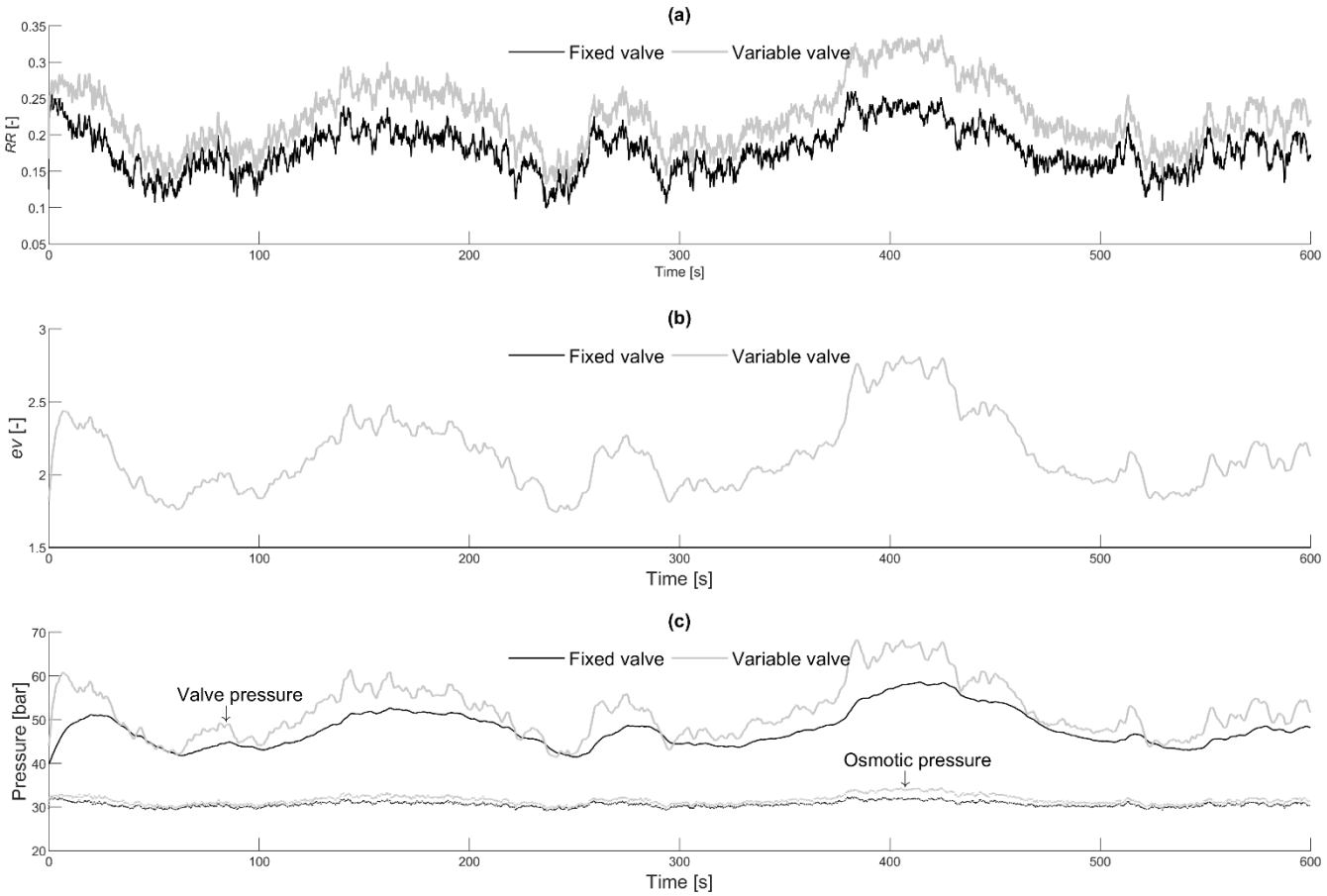

Figure 8: Recovery rate, friction losses factor and pressure.

brine assumes an almost steady trend, around a value of 1886 l/min, while in case of fixed valve the fluctuations are more accentuated with a higher mean value of 2163 l/min. Thus, the recovery rate in the first case is higher as shown in Figure 8a. The gap of the recovery rate is larger for higher current speeds. It follows that, with the same feed, a lower amount of brine needs to be disposed. Furthermore, a steady flowrate of the concentrate is associated to a constant velocity, resulting in an advantage for the resistance of the membrane if designed in the proper operational range. From the results of this case study, the variable valve configuration produces a higher production of freshwater with a better utilization of the feed. In both cases the energy extracted is enough to allow water production for current speeds above 1.5 m/s.

In Figure 8b the valve setting used as control variable for the variable valve is plotted. The mean value of the friction factor e_v in the active controlled configuration is 2.1450, which is higher than the constant value of 1.5 from the fixed valve setting. A higher valve resistance induces a higher-pressure difference across the valve as displayed in Figure 8c. The response of the osmotic pressure is very similar in both configurations, even if slightly smaller in the case of the fixed valve. It is important to notice that the osmotic pressure is not a constant value, but it depends on the concentration at the feed side and it has been assumed equal to a weighted average of feed concentration and the brine stream concentration.

6 CONCLUSION AND FUTURE WORK

In the present work the analysis of a reverse osmosis desalination powered by a horizontal axis tidal current turbine has been presented. A time-domain numerical model has been developed in order to simulate the system response to a turbulent current speed. The model couples the hydrodynamic model of the rotor, the positive displacement pump model and the RO membrane solution-diffusion model. The simplified system model is based on physical principles and can be used as a starting point to describe the dynamic behavior of the tidal driven reverse osmosis system.

Two variable speed configurations are proposed and compared. In the first one, a fixed setting for the opening position of the concentrate valve is defined; while in the second configuration, the valve setting was actively controlled in order to maximize the power capture from the turbine.

From the simulation results, the fixed valve configuration allows a higher operability and flexibility for a wider range of rotational speed and current speed. The operation of this configuration at higher tip speed ratios should be also analyzed to avoid possible cavitation issues. On the other hand, the variable

valve configuration maximizes the power extraction from the turbine and its utilization, making both the turbine and the membrane working in better conditions.

Future work involves validation of the results through hybrid modelling, combining physical test of the membrane and real-time numerical simulations of the tidal turbine hydrodynamics. In addition, the possibility to include energy recovery devices with the RO system will be explored.

References

Akash, B. A., & Mohsen, M. S. (1998). Potentials for development of hydro-powered water desalination in Jordan. *Renewable Energy*, *13*(4), 537–542.

Bartman, A. R., Christofides, P. D., & Cohen, Y. (2008). Nonlinear Model-Based Control of an Experimental Reverse Osmosis Water Desalination System, 6126–6136. https://doi.org/https://doi.org/10.3182/20090712-4-TR-2008.00146

Batten, W. M. J., Bahaj, A. S., Molland, A. F., & Chaplin, J. R. (2008). The prediction of the hydrodynamic performance of marine current turbines. *Renewable Energy*, *33*(5), 1085–1096. https://doi.org/10.1016/j.renene.2007.05.043

Bianchi, F. D., De Battista, H., & Mantz, R. J. (2007). *Wind Turbine Control Systems*. *Cleveland Clinic quarterly* (Vol. 26). Springer. https://doi.org/10.1007/1-84628-493-7

Cave, P. R., & Evans, E. M. (1984). *Tidal stream energy systems for isolated communities.*

Corsini, A., Tortora, E., & Cima, E. (2015). Preliminary assessment of wave energy use in an off-grid minor island desalination plant. *Energy Procedia*, *82*, 789–796. https://doi.org/10.1016/j.egypro.2015.11.813

DOW. (2013). Water & Process Solutions, FILMTEC ™ Reverse Osmosis Membranes: Technical Manual. *Dow Chemical Company*, 181. Retrieved from http://www.dow.com/en-us/water-and-process-solutions/products/reverse-osmosis#/accordion/F36C1D89-9385-480A-9242-575D600E6F81

Elimelech, M., & Phillip, W. A. (2011). The Future of Seawater and the Environment: Energy, Technology, and the Environment. *Science*, *333*(August), 712–718. https://doi.org/10.1126/science.1200488

Folley, M., & Whittaker, T. (2009). The cost of water from an autonomous wave-powered desalination plant. *Renewable Energy*, *34*(1), 75–81. https://doi.org/10.1016/j.renene.2008.03.009

Goundar, J. N., & Ahmed, M. R. (2013). Design of a horizontal axis tidal current turbine. *Applied Energy*, *111*, 161–174. https://doi.org/10.1016/j.apenergy.2013.04.064

Ling, C., Wang, Y., Min, C., & Zhang, Y. (2017). Economic evaluation of reverse osmosis desalination system coupled with tidal energy. *Frontiers in Energy*. https://doi.org/10.1007/s11708-017-0478-2

Ma, Q., & Lu, H. (2011). Wind energy technologies integrated with desalination systems: Review and state-of-the-art. *Desalination*, *277*(1–3), 274–280. https://doi.org/10.1016/j.desal.2011.04.041

Merritt, H. (1967). *Hydraulic Control Systems*. John Wiley & Sons. https://doi.org/10.1115/1.3601167

Mizutani, D. (2016). Sustainable Options for Desalination : A look into Renewable Energies and Brine Disposal by, (August).

Ning, S. A. (2014). A simple solution method for the blade element momentum equations with guaranteed convergence. *Wind Energy*, *17*(April 2013), 657–669. https://doi.org/10.1002/we

Rourke, F. O., Boyle, F., & Reynolds, A. (2010). Tidal energy update 2009. *Applied Energy*, *87*(2), 398–409. https://doi.org/10.1016/j.apenergy.2009.08.014

Slocum, A. H., Haji, M. N., Trimble, A. Z., Ferrara, M., & Ghaemsaidi, S. J. (2016). Integrated Pumped Hydro Reverse Osmosis systems. *Sustainable Energy Technologies and Assessments*, *18*, 80–99. https://doi.org/10.1016/j.seta.2016.09.003

Thomson, J., Talbert, J., Kilcher, L., Richmond, M., Talbert, J., DeKlerk, A., … Cienfuegos, R. (2013). Tidal turbulence spectra from a compliant mooring. *Proceedings of the 1st Marine Energy Technology Symposium*, *METS 2013*, 1–9.

Wijman, J. G., & Baker, R. W. (1995). The Solution Diffusion Model : A Review. *Journal of Membrane Science*.